Dual-Band Electrochromic Devices Utilizing Niobium Oxide Nanocrystals

Benjamin Z. Zydlewski[†] and Delia J. Milliron[*,‡,†]

[†]*Department of Chemistry, University of Texas at Austin, Austin, Texas 78712, United States*

[‡]*McKetta Department of Chemical Engineering, University of Texas at Austin, Austin, Texas 78712, United States*

E-mail: milliron@che.utexas.edu

Abstract

In this study we realize functioning electrochromic devices based on colloidal niobium oxide nanocrystals which show dual-band electrochromic behavior, with spectral selectivity between near-infrared and visible wavelengths. Minimally coloring vanadium oxide counter electrodes allow for full electrochromic devices that embody the dual-band electrochromic behavior of the niobium oxide component. The devices are fabricated using solution processing on both glass and flexible substrates, demonstrating that our platform has potential for the development of low-cost dual-band electrochromic devices for dynamic solar control in a variety of form factors and applications.

Keywords

electrochromic, colloidal nanocrystals, smart window, flexible film, solution processing, intercalation

Introduction

The optical properties of electrochromic materials modulate through the application of an electrical stimulus, allowing for dynamic control of transparency to light. Electrochromic smart windows that can modulate the transmittance allow for tuning of both the visible light and heat flux entering our spaces, which can be adapted based on climate conditions to reduce the power consumption of lighting, heating, and cooling systems.[1,2] The most heavily studied electrochromic material for smart windows is tungsten oxide, which generally shows broadband absorption across the visible and near-infrared (NIR) portions of the solar spectrum that can be ascribed to the formation of localized electronic states known as polarons.[3] Considering the NIR component of the solar irradiance accounts for almost half of the total energy coming from the sun, the ability to selectively block NIR light without impacting the visible transparency is advantageous to blocking excess heat entering through windows while still leveraging daylight. Dynamic window glazings that can reversibly modulate the transmittance of visible and NIR light independently have potential to further improve the energy savings of buildings by decoupling the influx of light and heat from solar radiation.[4,5]

Materials with selective electrochromism in NIR wavelength ranges are crucial to the development of dual-band electrochromic windows. NIR electrochromism was first achieved in doped metal oxide NCs due to the distinctive plasmonic absorption of free-charge carriers, which absorb primarily in the near to mid-infrared depending on doping levels. Capacitive electrochemical charging of doped metal oxide NCs such as Sb:SnO_2 and Sn:In_2O_3 alters the population of delocalized electrons in the NCs, allowing for tunability of the plasmonic extinction of near-infrared light.[6–9]

Dual-band electrochromism was first demonstrated by utilizing the plasmonic properties of Sn:In_2O_3 nanocrystals (NCs) embedded in a glassy niobium oxide matrix.[10] Visible and NIR light could be independently modulated based on the applied electrochemical potential, with the Sn:In_2O_3 NCs absorbing NIR light through plasmonic absorption and the niobium oxide leading to visible coloration due to polaronic absorption. The two-component approach

allows for the addition of a second coloration modality, which due to the differing reduction potentials of materials can be activated based on the electrochemical potential applied to the composite film.[11,12] A simplified approach would utilize a single material that has different coloration modes depending on the extent of reduction.

Both capacitive charging and cation intercalation can provide charge balance for injected electrons during the electrochemical reduction of transition metal oxide NCs, which can modulate the plasmonic or polaronic absorption depending on the extent of charge localization.[13–18] The ability to show both plasmonic absorption due to free charge carriers and polaronic absorption, indicative of charge localization, within a single material opens the door to single component dual-band electrochromics. Doped titanium oxide NCs have shown promise as single-component dual-band materials due to the ability to block NIR light through capacitive modulation of the plasmonic absorption, followed by an intercalation-driven phase transition leading to visible electrochromism.[15,16] Tungsten oxide NCs can be doped interstitially with small cations or with electrons arising from oxygen vacancies, leading to NIR plasmonic absorption. Dual-band behavior can be achieved through potential-dependent reduction, with low voltages leading to primarily NIR absorption and larger applied biases leading to visible coloration due to the intercalation of small cations.[17,18] While these materials are promising candidates for next-generation smart windows, they have drawbacks related to ultraviolet (UV) stability, non-color neutral coloration, and slow charging speeds associated with phase transitions. We believe similar nanostructuring and doping techniques can be applied to other oxides to develop new dual-band electrochromic materials.

Niobium oxides have received relatively little attention from the electrochromics community compared to other transition metal oxides due to low coloration efficiencies in both aqueous acidic electrolytes and nonaqueous lithium electrolytes.[19,20] Both amorphous and crystalline forms of niobium oxide transition from transparent to colored when reduced.[21,22] More recent research has shown that crystal phase and nanostructuring can significantly alter electrochromic performance, with orthorhombic Nb_2O_5 nanorods showing strong NIR

electrochromism with little, long wavelength visible coloration providing a blue tint[23] while amorphous Nb_2O_5 colors selectively at short wavelengths, taking a brown tint.[24] The crystal chemistry of niobium oxide is quite complex, with many different polymorphs that consist of varying arrangements of NbO_6 and NbO_7 subunits.[25] Niobium oxide NCs in the Wadsley-Roth shear phase, monoclinic $Nb_{12}O_{29}$, have been recently developed in our group which show potential dependent visible and NIR electrochromism with high optical modulation, making this an interesting new material to study in full electrochromic devices.[26–28] It was shown that the different sites occupied by lithium cations during ion intercalation influence the extent of electron localization, allowing for both plasmonic and polaronic absorption.[28] Reversible metal electrodeposition has recently been shown to allow for high visible light modulation, but it is unable to allow for selective NIR blocking.[29,30] The ability to modulate the transmittance in the visible and NIR selectively in a single component reduces the complexity of the device when compared to dual-band devices that utilize composite electrochromic electrodes or incorporate metal electrodeposition in addition to ion intercalation based systems.[31,32] Niobium oxide can also potentially alleviate issues associated with UV stability due to the wider bandgap reducing absorption of UV light from the sun and it shows more neutral coloration compared to tungsten oxide, making it more aesthetic for practial use.

A key advantage of NC-based electrochromics in general is the ability to produce colloidal inks that can be easily coated into thin films by solution processing techniques such as spin-coating and blade-coating. These lab-scale methods provide a stepping stone to the development of established large-scale manufacturing processes such as curtain coating and roll-to-roll processing on flexible substrates. Solution processing of thin films reduces production costs due to the ability to avoid ultra-high vacuum and high temperatures associated with more commonly used sputtering techniques to produce metal oxide thin films. Unlike typical sol-gel coating methods, the decoupling of the high-temperature synthesis of the NCs from the deposition of thin films allows for the use of substrates that have low melting points,

such as plastics.[13,24,33] Plastic substrates afford flexibility to the device, which can allow for fabrication by roll-to-roll processing and open new markets including retrofitting existing windows with dynamic window films and lamination into curved glass products.

An additional consideration when developing full electrochromic devices is the coloration of the counter electrode. In many devices, both electrodes are electrochromic, with the sum of the two leading to the observed color. However, in dual-band devices where selective NIR coloration is desired, an electrochromic counter electrode can negatively impact the spectral selectivity unless both electrodes color synergistically. The most commonly used counter electrode material is NiO, which colors broadly across the visible range under anodic (oxidative) charging.[3] If paired with a dual-band cathodic electrode, the visible coloration of the NiO would reduce the overall spectral selectively between NIR and visible light in the full device. To overcome this challenge, here we utilize optically passive counter electrodes composed of vanadium oxide, which show minimal coloration.[34]

In this study, we show that niobium oxide NCs can be utilized in dual-band electrochromic devices with high optical modulation and voltage-dependent spectral selectively between visible and NIR radiation when paired with vanadium oxide counter electrodes. Solution-processed thin films of the electrochromic materials afford the ability to produce rigid glass devices and flexible plastic devices, which we show have comparable performance. These prototype devices demonstrate the promise of colloidal NC-based electrochromics for the development of low-cost smart windows for next-generation, dual-band dynamic solar control.

Materials and Methods

Materials

Oleic acid (90%), N,N-dimethylformamide (DMF, 99.8%), nitrosonium tetrafluoroborate ($NOBF_4$, 95%), acetonitrile (99%), hexane (99%), isopropanol (99.5%), ethanol (99%), vanadium chloride (VCl_3, 99%), lithium perchlorate (99%), and propylene carbonate (PC, 99%)

were purchased from Sigma-Aldrich. Sodium oleate (>97%) was purchased from TCI. Ammonium niobium(V) oxalate (ANO, $NH_4[NbO(C_2O_4)_2(H_2O)_2]$) was provided by Companhia Brasileira de Metalurgia e Mineração (CBMM).

Nanocrystal Synthesis

Colloidal synthesis was used to make monoclinic $Nb_{12}O_{29}$ NCs, resulting in stable dispersions in hexane. The synthesis was modified from the method reported by Lu et al.[28] Specifically, 2.5 g of ANO and 0.75 g of sodium oleate were dissolved in 100 mL of oleic acid and heated to 120°C. The reaction mixture was then degassed using a Schlenk line for 1 hour under vaccuum to a pressure of 50 mtorr. The white mixture was then heated to 320°C under nitrogen flow and reacted for 4 hours. The reaction mixture turns bluish-green as the reaction proceeds. The mixture was cooled to room temperature and transfered to a nitrogen glovebox to prevent exposure to air. The NCs were isolated from any byproducts by washing with hexane and isopropanol followed by centrifugation at 7500 rpm for 5 minutes. The supernatant was discarded, leaving a blue solid that was redispersed in hexane. The washing process was repeated two more times by redispersing in hexane and flocculating with isopropanol. The final product is a light blue NC dispersion in hexane.

Electron Microscopy

Characterization of the NC morphology was done by dropping 10 μL of a 0.1 mg/mL NC dispersion in hexane on a carbon-coated Cu grid for imaging using scanning transmission electron microscopy (STEM). The NCs were imaged using a Hitachi S5500 scanning electron microscope in STEM mode.

XRD

Powder X-ray diffraction (XRD) was used to determine the crystal structure of the NCs. A Rigaku R-Axis Spider with a Cu Kα source was used to measure a dried NC powder sample

mounted on a cryoloop, which avoids possible texturing effects when analyzing substrate-deposited films.

Thin Film Deposition

Niobium oxide NC thin films were deposited using blade coating. Before deposition, the oleic acid ligands that coat the surface of the NCs were chemically stripped off using nitrosonium tetrafluoroborate ($NOBF_4$) to transfer the NCs into N,N-dimethylformamide (DMF) following a procedure previously reported.[26,35] The ligand-stripped NCs were washed five times through repeated flocculation with toluene followed by centrifugation and redispersion in clean DMF. The washed NCs were concentrated to 100 mg/mL in a 50:50 mixture of DMF and acetonitrile. ITO coated glass and poly(ethylene terephthalate) (PET) were washed by sonication in isopropanol for 30 minutes, dried under nitrogen flow, and then treated for 10 minutes in a Jelight Model No. 42 UVO cleaner. The concentrated NC ink was used to coat clean pieces of ITO coated glass or PET using an Elcometer 4340 motorized film applicator with a Leneta AB-86 Bird Applicator. A 50°C bed temperature and blade speed of 80 mm/s were used to deposit the niobium oxide NC thin films. For multiple layers the films were allowed to dry on the bed for 20 minutes followed by a secondary coatings using the same deposition conditions previously stated. The films were dried on a hotplate at 153°C for 20 minutes to remove residual solvent.

Vanadium oxide thin films were deposited using a modification of the method described by Zhao et al.[34] A 0.25 M VCl_3 solution in ethanol was blade coated on ITO glass or PET with a 65°C bed temperature and blade speed of 5 mm/s. Multiple layers could be deposited sequentially with 10 minute drying steps at 65°C between coats. The dried films of VCl_3 were oxidized with ozone for 1 hour inside a Jelight Model No. 42 UVO cleaner. The resulting amorphous vanadium oxide thin films were used as counter electrodes in electrochromic devices.

Spectroelectrochemistry

Spectroelectrochemistry of thin films was conducted inside an Ar glovebox to avoid air and moisture exposure. Thin films were immersed in 1.0 M $LiClO_4$ in propylene carbonate (PC) with a lithium foil counter and reference electrode. The potential of the thin films were controlled using a Biologic VMP3 potentiostat while monitoring the transmittance using an ASD Quality Spec Pro Vis-NIR spectrometer with fiber optic cables inside the glovebox. Chronoamperometry and chronopotentiometry were used to charge and discharge films to monitor their electrochromic response and charge storage capacity. Typical experiments involved monitoring the transmittance of a thin film during various potential step experiments to determine the potential window across which coloration occurs at NIR and visible wavelengths. The current response was used to calculate associated charge capacities that correspond to the different coloration states of the materials.

Electrochromic Device Fabrication

Before assembly, the vanadium oxide films were pre-lithiated by holding at 1.5 V vs Li/Li^+ in an electrolyte of 1.0 M $LiClO_4$ in PC. Following reduction, the vanadium oxide thin films were rinsed with dimethyl carbonate and allowed to dry. The thin films were coated with a gel electrolyte consisting of 1.0 M $LiClO_4$ in PC with 20 wt% dissolved poly(methyl methacrylate) (PMMA). Electrochromic devices were assembled by sandwiching the gel electrolyte and double-sided tape spacer (approximately 60 μm thick) between two ITO coated glass substrates – one coated with a niobium oxide NC film and the other with a vanadium oxide film. The edges of the assembled devices were sealed with epoxy to prevent exposure to air. Flexible devices using ITO-coated PET were fabricated in the same manner as rigid devices.

UV Stability

The stability to ultraviolet radiation (UV) was evaluated by prolonged exposure to a Spectroline ENF-280C 365 nm UV lamp. The transmittance of the films was measured prior to the UV exposure and then they were held under the UV lamp at a distance of 1 cm. The measured power of the lamp at this distance was 5.6 mW/cm^2. The films were coated with a small amount of electrolyte made of 1.0 M $LiClO_4$ in PC during the UV exposure to simulate the conditions in an electrochromic device.

Results and Discussion

Niobium oxide NCs were synthesized by adapting methods previously reported by Lu et al.[28] The NCs form through a heat-up colloidal synthesis reaction of ANO in oleic acid. The NCs are recovered from the reaction mixture and are dispersible in non-polar solvents such as hexane due to the colloidal stability afforded by the oleic acid ligands that cap their surfaces. Crystallinity and NC morphology were characterized using XRD and STEM (Figure 1). The organic ligands are chemically stripped from the NCs using $NOBF_4$ to improve electronic conductivity in deposited thin films and to create in an open, porous film morphology.[13] The thin films were deposited by blade coating, with variation in film thickness between 100 and 1500 nm accomplished through coating multiple layers or varying NC ink concentration. Film thickness was determined using stylus profilometry. Spectroelectrochemistry was used to study the electrochromism of the NC thin films. The NCs show a strong potential-dependent electrochromic response, with an initial decrease in transmittance primarily in the NIR, followed by a decrease in the visible transmittance upon further reduction to 1.5 V vs Li/Li^+ (Figure 1d). The electrochromic response matches well with what has been previously reported for $Nb_{12}O_{29}$ NCs.[26,28]

Full electrochromic devices function in an analogous way to a battery, with two electrodes that allow for the reversible movement of charge back and forth during coloring and bleaching.

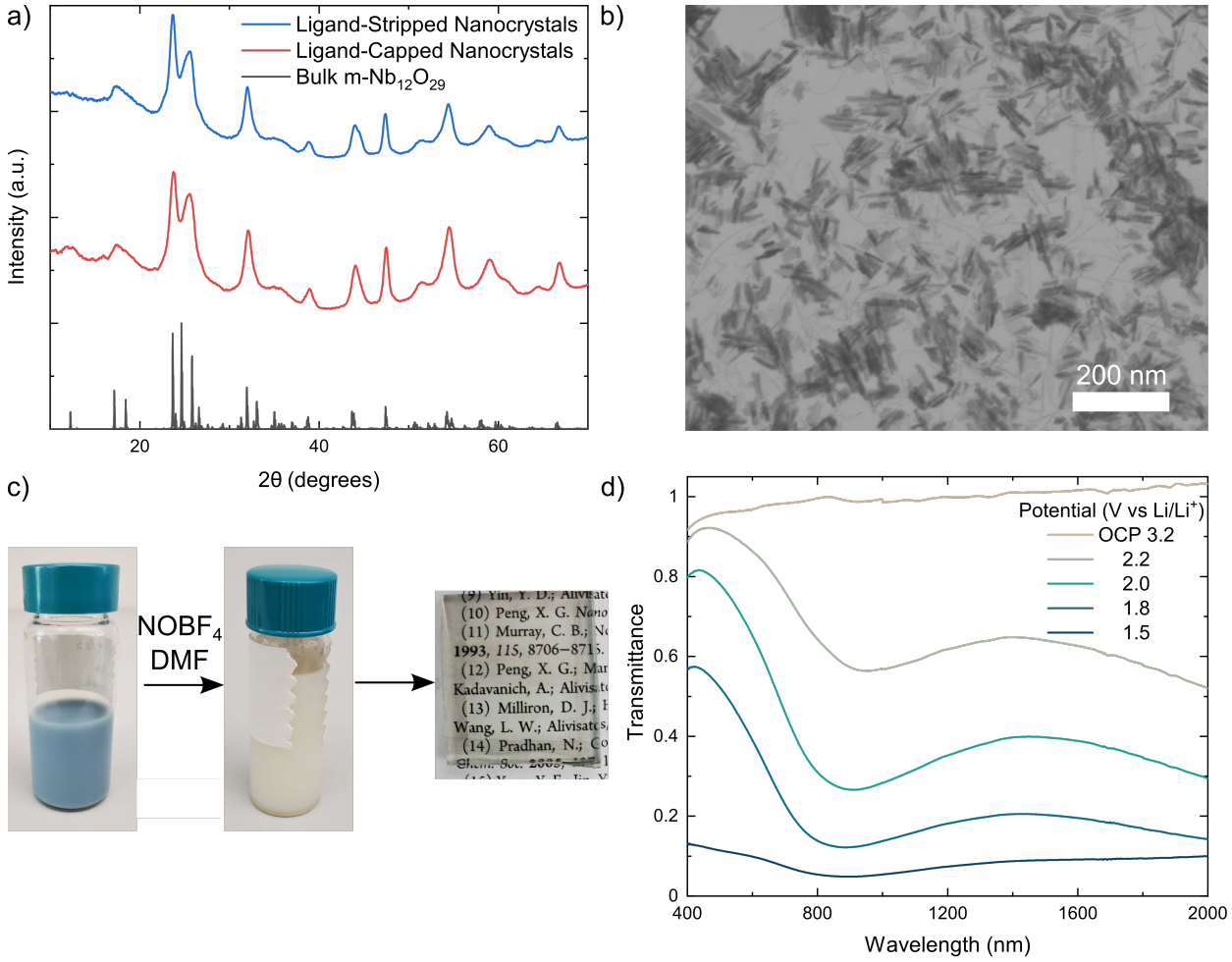

Figure 1: a) X-ray diffraction pattern of synthesized $Nb_{12}O_{29}$ NCs (offset for clarity) and reference pattern of bulk monoclinic-$Nb_{12}O_{29}$. b) STEM image of $Nb_{12}O_{29}$ NCs. c) Photographs showing the colloidal dispersions of NCs in hexane and DMF after chemical ligand striping using $NOBF_4$ and an ITO coated glass substrate supporting a niobium oxide NC thin film. d) Spectroelectrochemical characterization of a ∼500 nm thin film of $Nb_{12}O_{29}$ NCs deposited on ITO-coated glass. Transmittance is shown as a function of the applied electrochemical potential vs Li/Li^+ in an electrolyte containing 1.0 M $LiClO_4$ in PC. The film spectra are referenced to a background taken using a clean piece of ITO-coated glass.

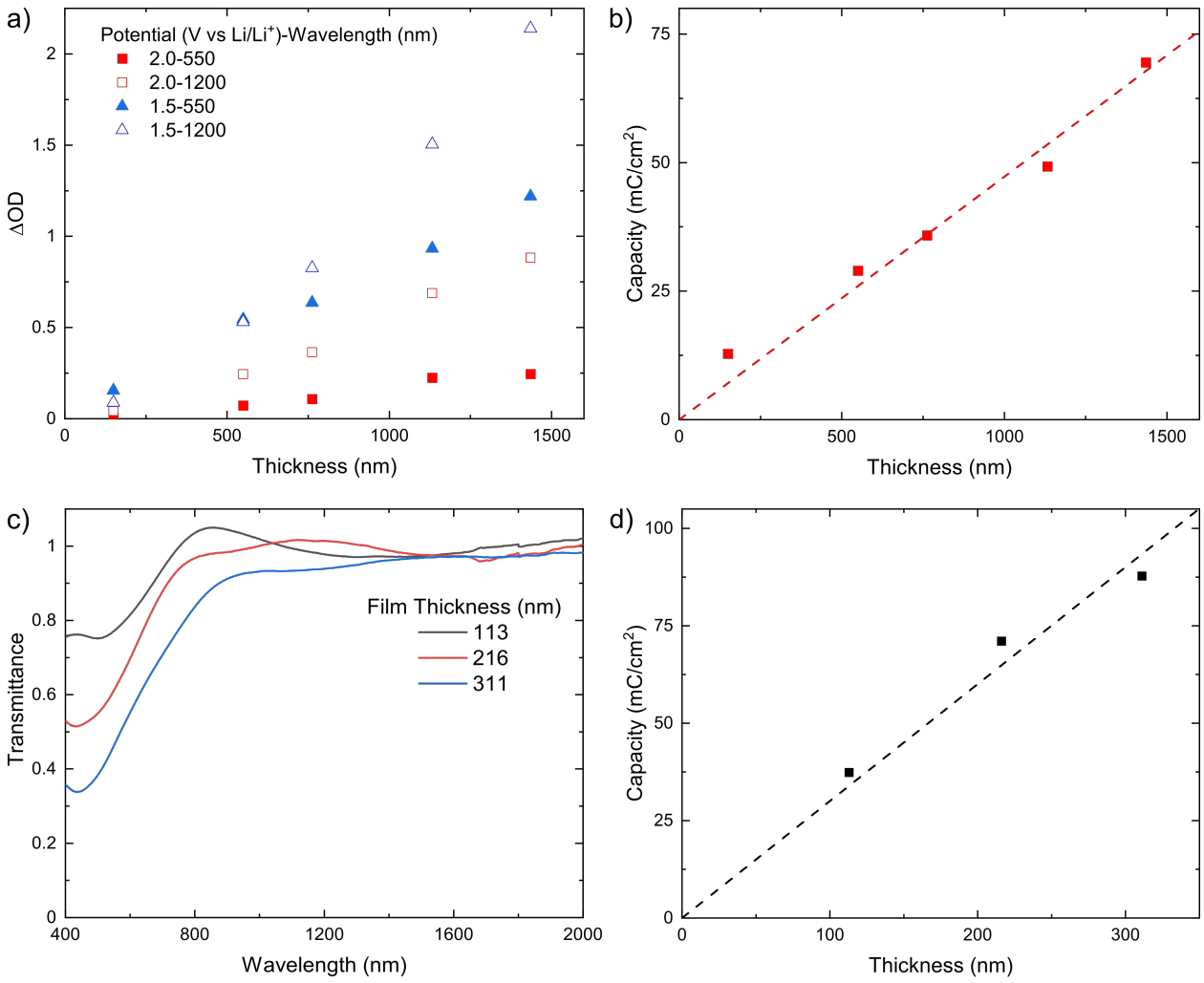

Figure 2: a) Change in optical density at 550 nm and 1200 nm wavelength of $Nb_{12}O_{29}$ NC thin films as a function of film thickness at various states of reduction relative to the bleached state. b) Charge capacity of $Nb_{12}O_{29}$ NC thin films as a function of film thickness measured using chronoamperometry at 1.5 V vs Li/Li^+. c) Transmittance of V_2O_5 films electrochemically reduced using chronoamperometry at 1.5 V vs Li/Li^+ in 1.0 M $LiClO_4$ in PC. d) Charge capacity of V_2O_5 thin films as a function of film thickness.

The two electrodes must have charge capacities that match to allow for full charging and discharging during operation of the device. The charge capacity and optical modulation of $Nb_{12}O_{29}$ NC films were analyzed based on variation in film thickness to determine optimum parameters for incorporation into full-cell devices. The change in optical density from the bleached state (ΔOD) was compared in both the infrared region (1200 nm) and the visible region (550 nm) to determine how the electrochromic response scales with film thickness (Figure 2a). The charge capacity as a function of film thickness scales linearly with a slope of 0.047 mC/cm^{2}nm, indicating that that the deposited material is contributing equally throughout the film thickness to the electrochemical capacity (Figure 2b).

To preserve the dual-band modulation in the full device, we sought an ion-storage electrode with minimal coloration to avoid interfering with the voltage-selective control over the NIR and visible transmittance afforded by the niobium oxide NCs. Vanadium oxide thin films were chosen due to their low coloration and high charge capacities.[34]

Vanadium oxide ion storage layers were deposited using a method modified from a procedure recently published.[34] The process involves solution processing of VCl_3 thin films by doctor blading from solutions of 0.25 M VCl_3 in ethanol. The films are oxidized by ozone to form amorphous vanadium oxide. Variation in film thickness of the vanadium oxide counter electrodes was accomplished by multi-layer deposition, similar to our approach to controlling thickness of the niobium oxide NC films. The charge storage capacity varied with film thickness in a linear fashion with a slope of 0.30 mC/cm^{2}nm, allowing for tunable matching to the working electrode for charge balance. At the greatest film thickness, the trend appears slightly sublinear, potentially indicating solid-state diffusion limitations on the charge capacity are approached with increased thickness in this range. Unfavorably, the visible transparency of the films when electrochemically reduced at 1.5 V vs Li/Li$^+$ diminished with increasing thickness (Figure 2c). This coloration is an important factor limiting the use of vanadium oxide electrodes to those with moderate charge capacity to avoid an unacceptable decrease in bleached state transmittance of the full device. The vanadium ox-

ide electrodes do show electrochromism, but the overall optical modulation is insignificant (Figure S1). The relationship between film thickness and charge capacity allowed us to determine conditions for overall charge balance, while minimizing the loss of transparency in the bleached state (Figure 2d).

Once optimum conditions for charge balance were determined, the working and counter electrodes were assembled into full-cell devices. To balance the overall transmittance change and bleached state transparency, film thicknesses of ∼500 nm and ∼150 nm were chosen for $Nb_{12}O_{29}$ NC and V_2O_5, respectively. This configuration allowed for overall charge capacities of the full devices between 25-30 mC/cm^2. The high coloration efficiency of the $Nb_{12}O_{29}$ NCs allows for a moderate thickness film that can be charge balanced by a thin V_2O_5 layer, which maximizes the bleached state transparency while still enabling strong coloration in the dark state. The devices were made by sealing the electrodes together with a doubled-sided tape acting as a spacer, with a layer of non-aqueous electrolyte sandwiched between (Figure 3a). The key advantage of the optically passive ion storage layer is the lack of significant coloration allows for the overall coloration of the full device to match closely to that of the half-cell measurements of the niobium oxide NC films. The device maintains the dual-band coloration, with minimal visible coloration below 1.0 V, but significant NIR coloration. Applying higher voltage drives the further reduction of the NCs, leading to more significant visible coloration (Figure 3b). The visible color of the device at each charge state shows blue tinting of the device during initial coloration due to the absorbance of red light. To quantify the NIR and visible selectivity as a function of the device potential we have tabulated the Solar Heat Gain Coefficient (SHGC), T_{NIR}, T_{vis}, and T_{Lum}. The SHGC is a metric of how much total energy passes through a window due to the transmittance of radiation from the sun, while T_{NIR} and T_{vis} are metrics of the transmittance of the NIR and visible portions of the solar spectrum, respectively. T_{Lum} is a measure of the visible transparency relative to the human eye based on the photopic luminosity function, which corrects the visible transparency for the sensitivity of the the eye as a function of wavelength. The explicit

functions used to calculate these values are shown in the Supporting Information.

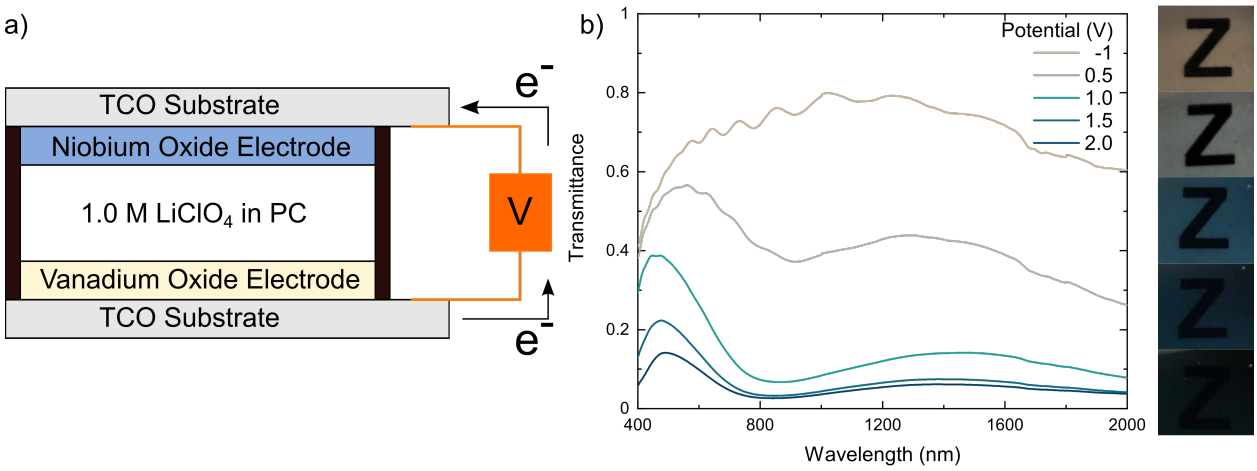

Figure 3: a) Schematic showing the components of the full electrochromic device incorporating niobium oxide NC and vanadium oxide electrodes. b) Transmittance vs wavelength of a rigid glass electrochromic device at various applied electrochemical potentials and corresponding photographs in room light with a white background. The device consists of a ~500 nm $Nb_{12}O_{29}$ NC film and a ~150 nm V_2O_5 film.

The advantage of $Nb_{12}O_{29}$ NCs is their dual-band electrochromic response, including the significant modulation of NIR apart from any extensive visible modulation. The spectral selectivity is quantitatively reflected in the difference between the modulation of T_{vis} and T_{NIR}, revealing selective control of the SHGC while daylight transmission remains substantial in the intermediate tinted states of the device (Table 1). The ΔT_{vis} and ΔSHGC between the bleached state at -1.0 V and the state at 0.5 V are 0.11 and 0.23, respectively. The intermediate states provide modes of the device that significantly reduce heat flux through the window while maintaining high visible transparency. This cool mode allows daylighting to reduce the need for electric lighting while still reducing cooling loads, a functionality which has been predicted to enable improved energy efficiency compared to traditional electrochromic devices and static windows.[5] In addition to the discrete potential settings shown in Figure 3, the device can be modulated continuously between the states, allowing for significant tunability of the ratio between the T_{vis} and the SHGC.

Solution-processability of the thin films affords key advantages for scalable and low-cost

Table 1: Performance Metrics

Potential (V)	T_{vis}	T_{Lum}	T_{NIR}	SHGC
-1.0	0.63	0.66	0.75	0.69
0.5	0.52	0.55	0.41	0.46
1.0	0.29	0.31	0.10	0.19
1.5	0.15	0.17	0.05	0.10
2.0	0.10	0.12	0.04	0.07

manufacturing and opens up options for the choice of substrates. Simple scaling to larger area films is achieved with blade coating, which allowed us to demonstrate 10x10 cm^2 devices that show comparable performance to smaller-scale devices (Figure S2). Table S1 shows a comparison between small and large area devices. They have similar charge densities and T_{vis} modulation, but there is a significant difference between the modulation of T_{NIR} and SHGC due to the difference in ITO substrate used. The large area device uses 30 Ohm/square ITO which has lower NIR transparency compared to the 60 Ohm/square ITO used in the smaller area devices, which results in the lower bleach state transmittance to NIR light in the 10x10 cm^2 device. The lack of any high-temperature processing also permits the use of plastic substrates. The same methods used to fabricate thin films on glass were used for PET substrates. Thin films of $Nb_{12}O_{29}$ NCs show comparable electrochromism on ITO-coated PET substrates as on glass (Figure S3). Vanadium oxide counter electrodes were deposited on ITO-coated PET the same way as on glass substrates. The full devices were assembled by coating one electrode with the gel electrolyte and then sandwiching the second electrode together with the gel electrolyte in between. Double-sided tape acts as a spacer to prevent the two electrodes from shorting, with the gel electrolyte occupying the gap between the electrodes. Flexible devices show similar performance to those of the glass devices (Figure 4), demonstrating the versatility of colloidal NC electrochromics. An in depth comparison of the performance is included in Table 1. The dark state coloration is slightly less than that of the glass device due to slightly lower charge capacities associated with lower film thicknesses.

In addition to the effective dual-band optical modulation of the electrochromic devices, they are also stable with repeated cycling between the bleached and colored states. A glass

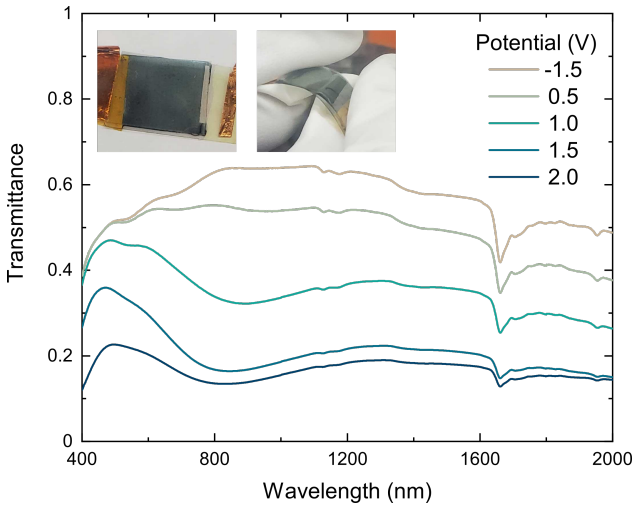

Figure 4: a) Transmittance of a flexible device as a function of applied electrochemical potential. Inset images show the coloration and flexibility of the device. The niobium oxide layer is ∼350 nm thick and the vanadium oxide layer is ∼150 nm thick.

device was cycled between 2.5 V and -2.5 V 1000 times using chronopotentiometry with a current density of 0.18 mA/cm^2, which shifts between states in approximately 2 minutes. The device performance before and after cycling shows minimal degradation (Figure S4 and Table S2). There is a 5.2% decrease in the modulation of T_{vis} and a 2.3% decrease in the modulation of the SHGC between the bleached and colored states. These results suggest that our niobium oxide-based electrochromic devices can provide not only high performance, but long term cycling stability. Our results show the promise of niobium oxide as an alternative material to the more commonly studied tungsten oxide in high performance electrochromic devices, which can allow for selective modulation of infrared and visible transmittance.

A secondary advantage of niobium oxide over tungsten oxide is the wider bandgap. Tungsten oxide suffers from deteriorating photochromic effects when exposed to UV radiation from the sun. The photochromism is the result of bandgap absorption which generates holes in the valance band that can readily oxidize molecules in the electrolyte. The optical bandgap of various forms of tungsten oxide are between 2.6-2.8 eV, which causes them to strongly absorb UV radiation from the sun, leading to proton-coupled electron transfer reactions that darken the tungsten oxide and degrade the electrolyte.[36] Monoclinic $Nb_{12}O_{29}$ has a larger

optical bandgap of around 4.0 eV, which is outside the range of UV radiation from the sun, preventing the photochromic degradation common in tungsten oxides.[37] We demonstrated the UV stability of the niobium oxide NC films through prolonged exposure to UV radiation from a 365 nm lamp. The stability was compared to a Cs:WO_3 NC film, showing the photochromic degradation that plagues the lower bandgap material, which can be exacerbated by the high interfacial contact area between the NCs and electrolyte (Figure 5). (Experimental details of the synthesis and characterization of the Cs:WO_3 NCs are reported in a previous publication.[17]) As holes in the valance band oxidize molecules in the electrolyte, electrons populate the conduction band and lead to increased absorption in the NIR. Niobium oxide NCs have superior resistance to this degradation mode due to their much larger bandgap, resulting in negligible change in transmittance after prolonged exposure.

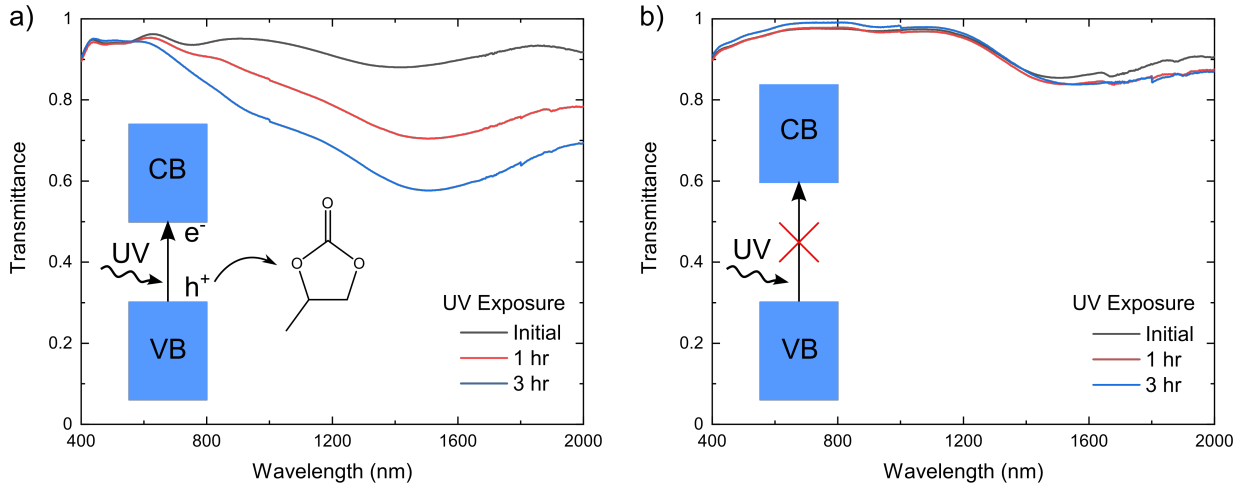

Figure 5: a) Transmittance spectra of Cs:WO_3 NC film at varying amounts of UV radiation exposure. b) Transmittance spectra of $Nb_{12}O_{29}$ NC film at varying amounts of UV radiation exposure. Both films were in contact with 1.0 M $LiClO_4$ in PC during the UV exposure. The inset schemes show the mechanism of photochromic degradation.

Conclusions and Outlook

We have developed electrochromic devices using solution-processable colloidal NCs that allow for both rigid and flexible substrates using niobium oxide as the primary active elec-

trochromic material. Vanadium oxide thin films were utilized as opitcally passive counter electrodes to preserve the spectral selectivity afforded by the $Nb_{12}O_{29}$ NCs, while allowing for charge balance for reversible cycling between colored and bleached states. The devices show a high degree of spectral selectivity between visible and infrared light, allowing for selective modulation of the SHGC at intermediate states of charge while maintaining high visible transparency. Colloidal NCs offer enhanced electrochromic functionality by precisely controlled composition and structure, like these monoclinic $Nb_{12}O_{29}$ shear phase NCs, which are not readily accessed in sputtered thin films. Owing to their low-temperature, solution processability, NCs also can reduce production costs associated with film fabrication. The performance of dual-band electrochromic devices could be enhanced through the development of complementary anode materials that show similar NIR and visible selectivity to improve the coloration and potentially further improve color neutrality. We believe further development of colloidal NC-based electrochromic windows can lead to significant cost savings in the production of high-performance dynamic smart windows, to enable broad deployment in new construction, retrofitting, and transportation, aiming to substantially reduce energy usage.

Supporting Information

The supporting information includes the following: Descriptions of T_{vis}, T_{Lum}, T_{NIR}, and SHGC; Electrochromism of vanadium oxide thin films; Electrochromic Performance of 10x10 cm^2 device; Electrochromism of $Nb_{12}O_{29}$ NCs on ITO-coated PET substrate; Cycling performance of electrochromic device; Device performance comparison table; Cycling Stability Performance Metrics.

Acknowledgement

The authors acknowledge support from Eastman Chemical Company and the Welch Foundation (F-1848). The authors would like to acknowledge Arianna Doss during her time in the Welch Summer Scholars Program where she assisted the UV exposure experiments.

References

(1) Cannavale, A.; Martellotta, F.; Cossari, P.; Gigli, G.; Ayr, U. Energy savings due to building integration of innovative solid-state electrochromic devices. *Appl. Energy* **2018**, *225*, 975–985.

(2) Tällberg, R.; Jelle, B. P.; Loonen, R.; Gao, T.; Hamdy, M. Comparison of the energy saving potential of adaptive and controllable smart windows: A state-of-the-art review and simulation studies of thermochromic, photochromic and electrochromic technologies. *Sol. Energy Mater. Sol. Cells* **2019**, *200*, 109828.

(3) Niklasson, G. A.; Granqvist, C. G. Electrochromics for smart windows: thin films of tungsten oxide and nickel oxide, and devices based on these. *J. Mater. Chem.* **2007**, *17*, 127–156.

(4) DeForest, N.; Shehabi, A.; O'Donnell, J.; Garcia, G.; Greenblatt, J.; Lee, E. S.; Selkowitz, S.; Milliron, D. J. United States energy and CO2 savings potential from deployment of near-infrared electrochromic window glazings. *Build Environ.* **2015**, *89*, 107–117.

(5) DeForest, N.; Shehabi, A.; Selkowitz, S.; Milliron, D. J. A comparative energy analysis of three electrochromic glazing technologies in commercial and residential buildings. *Appl. Energy* **2017**, *192*, 95–109.

(6) zum Felde, U.; Haase, M.; Weller, H. Electrochromism of Highly Doped Nanocrystalline SnO_2:Sb. *J. Phys. Chem. B* **2000**, *104*, 9388–9395.

(7) Pflughoefft, M.; Weller, H. Spectroelectrochemical Analysis of the Electrochromism of AntimonyDoped Nanoparticulate Tin Dioxide Electrodes. *J. Phys. Chem. B* **2002**, *106*, 10530–10534.

(8) Garcia, G.; Buonsanti, R.; Runnerstrom, E. L.; Mendelsberg, R. J.; Llordes, A.; Anders, A.; Richardson, T. J.; Milliron, D. J. Dynamically Modulating the Surface Plasmon Resonance of Doped Semiconductor Nanocrystals. *Nano Lett.* **2011**, *11*, 4415–4420.

(9) Zandi, O.; Agrawal, A.; Shearer, A. B.; Reimnitz, L. C.; Dahlman, C. J.; Staller, C. M.; Milliron, D. J. Impacts of surface depletion on the plasmonic properties of doped semiconductor nanocrystals. *Nat. Mater* **2018**, *17*, 710–717.

(10) Llordés, A.; Garcia, G.; Gazquez, J.; Milliron, D. J. Tunable near-infrared and visible-light transmittance in nanocrystal-in-glass composites. *Nature* **2013**, *500*, 323–326.

(11) Kim, J.; Ong, G. K.; Wang, Y.; LeBlanc, G.; Williams, T. E.; Mattox, T. M.; Helms, B. A.; Milliron, D. J. Nanocomposite architecture for rapid, spectrally-selective electrochromic modulation of solar transmittance. *Nano Lett.* **2015**, *15*, 5574–5579.

(12) Gu, H.; Guo, C.; Zhang, S.; Bi, L.; Li, T.; Sun, T.; Liu, S. Highly efficient, near-infrared and visible light modulated electrochromic devices based on polyoxometalates and $W_{18}O_{49}$ nanowires. *ACS Nano* **2018**, *12*, 559–567.

(13) Heo, S.; Kim, J.; Ong, G. K.; Milliron, D. J. Template-Free Mesoporous Electrochromic Films on Flexible Substrates from Tungsten Oxide Nanorods. *Nano Lett.* **2017**, *17*, 5756–5761.

(14) Giannuzzi, R.; Scarfiello, R.; Sibillano, T.; Nobile, C.; Grillo, V.; Giannini, C.; Cozzoli, P. D.; Manca, M. From capacitance-controlled to diffusion-controlled electrochromism in one-dimensional shape-tailored tungsten oxide nanocrystals. *Nano Energy* **2017**, *41*, 634–645.

(15) Dahlman, C. J.; Tan, Y.; Marcus, M. A.; Milliron, D. J. Spectroelectrochemical Signatures of Capacitive Charging and Ion Insertion in Doped Anatase Titania Nanocrystals. *J. Am. Chem. Soc.* **2015**, *137*, 9160–9166.

(16) Zhang, S.; Cao, S.; Zhang, T.; Lee, J. Y. Plasmonic Oxygen-Deficient TiO2-x Nanocrystals for Dual-Band Electrochromic Smart Windows with Efficient Energy Recycling. *Adv. Mater.* **2020**, *32*, 2004686.

(17) Zydlewski, B. Z.; Lu, H.-C.; Celio, H.; Milliron, D. J. Site-Selective Ion Intercalation Controls Spectral Response in Electrochromic Hexagonal Tungsten Oxide Nanocrystals. *J. Phys. Chem. C* **2022**, *126*, 14537–14546.

(18) Fortunato, J.; Zydlewski, B. Z.; Lei, M.; Holzapfel, N. P.; Chagnot, M.; Mitchell, J. B.; Lu, H.-C.; Jiang, D.-e.; Milliron, D. J.; Augustyn, V. Dual-Band Electrochromism in Hydrous Tungsten Oxide. *ACS Photonics* **2023**, *10*, 3409–3418.

(19) Mujawar, S. H.; Inamdar, A. I.; Patil, S. B.; Patil, P. S. Electrochromic properties of spray-deposited niobium oxide thin films. *Solid State Ion.* **2006**, *177*, 3333–3338.

(20) He, J.; You, L.; Tran, D. T.; Mei, J. Low-Temperature Thermally Annealed Niobium Oxide Thin Films as a Minimally Color Changing Ion Storage Layer in Solution-Processed Polymer Electrochromic Devices. *ACS Appl. Mater. Interfaces* **2019**, *11*, 4169–4177.

(21) Özer, N.; Barreto, T.; Büyüklimanli, T.; Lampert, C. M. Characterization of sol-gel deposited niobium pentoxide films for electrochromic devices. *Sol. Energy Mater. Sol. Cells* **1995**, *36*, 433–443.

(22) Maček, M.; Orel, B. Electrochromism of sol–gel derived niobium oxide films. *Sol. Energy Mater. Sol. Cells* **1998**, *54*, 121–130.

(23) Ong, G. K.; Saez Cabezas, C. A.; Dominguez, M. N.; Skjærvø, S. L.; Heo, S.; Milliron, D. J. Electrochromic Niobium Oxide Nanorods. *Chem. Mater.* **2020**, *32*, 468–475.

(24) Llordés, A.; Wang, Y.; Fernandez-Martinez, A.; Xiao, P.; Lee, T.; Poulain, A.; Zandi, O.; Saez Cabezas, C. A.; Henkelman, G.; Milliron, D. J. Linear topology in amorphous metal oxide electrochromic networks obtained via low-temperature solution processing. *Nat. Mater.* **2016**, *15*, 1267–1273.

(25) Nico, C.; Monteiro, T.; Graça, M. P. F. Niobium oxides and niobates physical properties: Review and prospects. *Prog. Mater. Sci.* **2016**, *80*, 1–37.

(26) Lu, H.-C.; Ghosh, S.; Katyal, N.; Lakhanpal, V. S.; Gearba-Dolocan, I. R.; Henkelman, G.; Milliron, D. J. Synthesis and Dual-Mode Electrochromism of Anisotropic Monoclinic $Nb_{12}O_{29}$ Colloidal Nanoplatelets. *ACS Nano* **2020**, *14*, 10068–10082.

(27) Lu, H.-C.; Zydlewski, B. Z.; Tandon, B.; Shubert-Zuleta, S. A.; Milliron, D. J. Understanding the Role of Charge Storage Mechanisms in the Electrochromic Switching Kinetics of Metal Oxide Nanocrystals. *Chem. Mater.* **2022**, *34*, 5621–5633.

(28) Lu, H.-C.; Katyal, N.; Henkelman, G.; Milliron, D. J. Controlling the Shape Anisotropy of Monoclinic $Nb_{12}O_{29}$ Nanocrystals Enables Tunable Electrochromic Spectral Range. *J. Am. Chem. Soc.* **2021**, *143*, 15745–15755.

(29) Strand, M. T.; Hernandez, T. S.; Danner, M. G.; Yeang, A. L.; Jarvey, N.; Barile, C. J.; McGehee, M. D. Polymer inhibitors enable >900 cm2 dynamic windows based on reversible metal electrodeposition with high solar modulation. *Nat. Energy* **2021**, *6*, 546–554.

(30) Guo, X.; Chen, S.; Poh, W. C.; Chen, J.; Jiang, F.; Tan, M. W. M.; Lee, P. S. Solid-State and Flexible Black Electrochromic Devices Enabled by Ni-Cu Salts Based Organohydrogel Electrolytes. *Adv. Mater. Interfaces* **2023**, *10*, 2300061.

(31) Pugliese, M.; Scarfiello, R.; Prontera, C. T.; Giannuzzi, R.; Bianco, G. V.; Bruno, G.; Carallo, S.; Mariano, F.; Maggiore, A.; Carbone, L.; Gigli, G.; Maiorano, V. Visible Light–Near-Infrared Dual-Band Electrochromic Device. *ACS Sustain. Chem. Eng.* **2023**, *11*, 9601–9612.

(32) Kim, J.; Shin, D.; Son, M.; Lee, C. S. High Optical Contrast of Quartet Dual-Band Electrochromic Device for Energy-Efficient Smart Window. *ACS Appl. Mater. Interfaces* **2023**, *15*, 13249–13257.

(33) Zhang, L.; Chao, D.; Yang, P.; Weber, L.; Li, J.; Kraus, T.; Fan, H. J. Flexible Pseudocapacitive Electrochromics via Inkjet Printing of Additive-Free Tungsten Oxide Nanocrystal Ink. *Adv. Energy Mater.* **2020**, *10*, 2000142.

(34) Zhao, W.; Wang, J.; Tam, B.; Pei, P.; Li, F.; Xie, A.; Cheng, W. Macroporous Vanadium Oxide Ion Storage Films Enable Fast Switching Speed and High Cycling Stability of Electrochromic Devices. *ACS Appl. Mater. Interfaces* **2022**, *14*, 30021–30028.

(35) Dong, A.; Ye, X.; Chen, J.; Kang, Y.; Gordon, T.; Kikkawa, J. M.; Murray, C. B. A Generalized Ligand-Exchange Strategy Enabling Sequential Surface Functionalization of Colloidal Nanocrystals. *J. Am. Chem. Soc.* **2011**, *133*, 998–1006.

(36) Wang, Y.; Kim, J.; Gao, Z.; Zandi, O.; Heo, S.; Banerjee, P.; Milliron, D. J. Disentangling Photochromism and Electrochromism by Blocking Hole Transfer at the Electrolyte Interface. *Chem. Mater.* **2016**, *28*, 7198–7202.

(37) Ohsawa, T.; Okubo, J.; Suzuki, T.; Kumigashira, H.; Oshima, M.; Hitosugi, T. An n-Type Transparent Conducting Oxide: $Nb_{12}O_{29}$. *J. Phys. Chem. C* **2011**, *115*, 16625–16629.

TOC Graphic